Modeling and Analysis of Time Response Parameters of a PMSM-Based Electric Vehicle with PI and PID Controllers

M. Yerri Veeresh
Department of EEE, Jawaharlal Nehru Technological University Anantapur, Anantapuramu, India and Santhiram Engineering College, Nandyal, India
saiveerushamu8@gmail.com

V. Naga Bhaskar Reddy
Department of EEE
Rajeev Gandhi Memorial College of Engineering and Technology, Nandyal, India
chaitu.bhaskar@gmail.com

R. Kiranmayi
Department of EE
Jawaharlal Nehru Technological University Anantapur
Anantapuramu, India
kiranmayi0109@gmail.com

Received: 9 September 2022 | Revised: 26 September 2022 and 4 October 2022 | Accepted: 9 October 2022

Abstract-This paper presents the mathematical modeling of a vector-controlled Permanent Magnet Synchronous Motor (PMSM) drive with either a Proportional Integral (PI) controller or a Proportional Integral Derivative (PID) controller as a propulsion system for an Electric Vehicle (EV). Most commercial drives use a standard PI controller as a speed regulator. The vector control system model consists of the PMSM, a PWM inverter, the speed controller, and vehicle dynamics for speed control. The performance analysis of the drive is evaluated under transient conditions for settling time, rise time, steady state error of speed, and the vehicle's acceleration at the wheel axle for specifically designated values validated by MATLAB/Simulink.

Keywords-Permanent Magnet Synchronous Motor (PMSM); electric vehicle dynamics; Proportional Integral (PI) controller; Proportional Integral Derivative (PID) controller

I. INTRODUCTION

In recent years, several situations related to the environment have led to reduced carbon emissions from vehicles. Electric Vehicles (EVs) can be alternatives to traditional SI or CI engine automotives [1-2]. PMSMs have been used in various industrial applications like CNC machines, industrial robotics, air-conditioners, washing machines, wind power generation systems, EVs, etc. The PMSMs are more suitable in EVs due to their high efficiency, high power/torque density, smaller size, high torque/weight ratio, and maintenance-free operation [3]. Better dynamic responsiveness and fewer torque ripples are provided by a vector-controlled PMSM drive, which needs a constant switching frequency. The outer loop speed control significantly impacts system performance [4].

The PI controller performs well under steady-state conditions. A lot of approaches have been proposed for the tuning of the PI controller. The Ziegler-Nichols method is the most popular, which dispenses with the need for a system design and control parameters [5]. The PI and PID controllers are simple and effective, consequently, they are often used for the control of the PMSM systems [6]. Controlling of a Battery EV (BEV) is not a simple task as the EV is essentially time-variant. The EV's primary limiting factor is the short running distance (range) per battery charge. Another limiting factor is its acceleration time to reach the maximum speed limit [7]. The EV dynamics must be suitably selected to achieve better performance.

II. VEHICLE DYNAMICS

The performance of vehicle modeling is initially obtained by the tractive effort equation. The force that drives the vehicle forward and is transmitted to the ground through the drive wheels is known as the tractive effort. This force has to overcome the rolling resistance force, aerodynamic drag force, and the elements of the vehicle's weight (including payload) acting down to the slope. It also accomplishes the force required to accelerate the vehicle for the linear and angular motion of drive wheels [7-8]. The tractive force and the corresponding force equations depend upon the vehicle dynamics, shape, size, and structure parameters, such as rolling resistance coefficient, air density, drag coefficient, gear ratio and gear efficiency, wheel radius, etc., are illustrated in Figure 1 of [9]. The respective equations for Rolling Resistance Force F_{rr}, Aerodynamic Drag Force F_{ad}, Hill Climbing Force F_{hc}, Acceleration Force F_{la}, and Angular Acceleration Force F_{wa} are respectively given by:

$$F_{rr} = \mu_{rr} * m * g \quad (1)$$

Corresponding author: M. Yerri Veeresh

$$F_{ad} = \frac{1}{2} * \rho * A * C_d * v^2 \quad (2)$$

$$F_{hc} = m * g * \sin\psi \quad (3)$$

$$F_{la} = m * a \quad (4)$$

$$F_{wa} = I\frac{G^2}{\eta_g r^2} \quad (5)$$

The total tractive force necessary to drive the vehicle is the sum of all forces:

$$F_{te} = F_{rr} + F_{ad} + F_{hc} + F_{la} + F_{wa} \quad (6)$$

The tractive torque corresponding to the tractive force with wheel radius r, is given by:

$$T_R = F_{te} * r \quad (7)$$

The speed and torque at the axle of the wheel are given by:

$$\omega_{axle} = \frac{\omega_e}{G} \quad (8)$$

$$T_{axle} = G\eta_G T_e \quad (9)$$

The vehicle equations are used to understand the vehicle dynamics for different force inputs [10]. The mathematical model of the speed-toque equation of the vehicle at the axle of the wheels is given by:

$$\omega_{axle} = \int \frac{1}{\left(mr^2 + \frac{G^2}{\eta_G} J\right)} [T_{axle} - T_R]\, dt \quad (10)$$

The specifications of the vehicle chassis chosen for the simulation are given in Table I.

TABLE I. VEHICLE CHASSIS SPECIFICATIONS

Parameter	Quantity
Net mass, m	1200Kg
Area of frontal surface, A	2.2m2
Gear ratio, G	2
Rolling coefficient, μ_{rr}	0.01
Gear efficiency, η_G	0.9
Wheel radius, r	0.2m
Drag coefficient, C_d	0.26
Slope angle, ψ	0^o

III. MATHEMATICAL MODEL OF THE PERMANENT MAGNET SYNCHRONOUS MOTOR

A three-phase salient-pole sinusoidal wave shape back EMF PMSM with 87.75Nm, 560Vdc, and 3000rpm preset model parameters was designed mathematically. The model specifications are given in Table II. The mathematical model of the PMSM is given in (11)-(22). The rotor reference frame is chosen because the rotor magnet's position will be determined independent of the stator phase voltages, instantaneous induced phase EMFs, stator phase currents, and torque of the machine [11]. For synchronous motors, the rotating speed of the rotor and the space vector of the rotor flux are both equal to the rotating rate of the reference frame $\omega_a = \omega_r = \omega$ [12-13].

In the rotor reference frame, the stator q and d axes voltage equations in terms of flux linkages are:

$$V_{qs} = R_q i_{qs} + \frac{d\varphi_{qs}}{dt} + \omega_r \varphi_{ds} \quad (11)$$

$$V_{ds} = R_d i_{ds} + \frac{d\varphi_{ds}}{dt} - \omega_r \varphi_{qs} \quad (12)$$

The stator flux linkages are given by:

$$\varphi_{qs} = L_q i_{qs} \quad (13)$$

$$\varphi_{ds} = L_d i_{ds} + L_m i_f \quad (14)$$

TABLE II. PMSM SPECIFICATIONS

Parameter	Value
Stator phase resistance, R_s ($R_d = R_q = R_s$)	0.05Ω
d-axis inductance, L_d	0.0007552H
q-axis inductance, L_q	0.0008348H
Flux linkage, φ_{af}	0.192 Wb-turn
Inertia, J	0.011Kgm^2
Viscous damping, B	0.001417Nms
Pole pairs, P	4
Static friction, T_f	0Nm

The stator voltage equations in terms of electrical parameters are obtained by substituting the flux linkages in the stator voltage equations as:

$$\begin{bmatrix} V_{qs} \\ V_{ds} \end{bmatrix} = \begin{bmatrix} R_q + \frac{dL_q}{dt} & \omega_r L_d \\ -\omega_r L_q & R_d + \frac{dL_d}{dt} \end{bmatrix} \begin{bmatrix} i_{qs} \\ i_{ds} \end{bmatrix} + \begin{bmatrix} \omega_r L_m i_f \\ 0 \end{bmatrix} \quad (15)$$

The electromagnetic torque is given by:

$$T_e = \frac{3}{2}\frac{P}{2}\left(\varphi_{ds} i_{qs} - \varphi_{qs} i_{ds}\right) \quad (16)$$

The torque equation in terms of inductances and currents upon the substitution of flux linkages is given by [14]:

$$T_e = \frac{3P}{4}\left\{\varphi_{af} i_{qs} + \left(L_d - L_q\right) i_{qs} i_{ds}\right\} \quad (17)$$

where φ_{af} is the rotor flux linkage that links the stator and is given by:

$$\varphi_{af} = L_m i_f \quad (18)$$

The angular speed ω_e and the instantaneous angle of the rotor θ_r of the machine are given by:

$$\omega_e = \frac{P}{2}\left[\frac{1}{Js+B}\right][T_e - T_m] \quad (19)$$

$$\theta_r = \int_0^t \omega_e(t)\, dt + \theta_r(0) \quad (20)$$

The stator q and d axes currents for a balanced three-phase operation are given by:

$$\begin{bmatrix} i_{qs} \\ i_{ds} \end{bmatrix} = \frac{2}{3}\begin{bmatrix} \cos\theta_r & \cos\left(\theta_r - \frac{2\pi}{3}\right) & \cos\left(\theta_r + \frac{2\pi}{3}\right) \\ \sin\theta_r & \sin\left(\theta_r - \frac{2\pi}{3}\right) & \sin\left(\theta_r + \frac{2\pi}{3}\right) \end{bmatrix} \begin{bmatrix} i_a \\ i_b \\ i_c \end{bmatrix} \quad (21)$$

The abc-to-dq transformation equations for stator voltages are given by:

$$\begin{bmatrix} v_{qs} \\ v_{ds} \end{bmatrix} = \frac{2}{3}\begin{bmatrix} \cos\theta_r & \cos\left(\theta_r - \frac{2\pi}{3}\right) & \cos\left(\theta_r + \frac{2\pi}{3}\right) \\ \sin\theta_r & \sin\left(\theta_r - \frac{2\pi}{3}\right) & \sin\left(\theta_r + \frac{2\pi}{3}\right) \end{bmatrix} \begin{bmatrix} v_a \\ v_b \\ v_c \end{bmatrix} \quad (22)$$

IV. PROPOSED SYSTEM MODEL WITH PI AND PID CONTROLLER

For applications in control theory, the Proportional (P), the PI, and the PID controllers are the most commonly used controllers. As illustrated in Figure 1, the PI controller will affect the performance of the system by increasing the system's order by one and by reducing steady state error, disturbance signal rejection, and relative stability. The system's sensitivity with respect to parameters also decreases [15]. The transfer function of the PI controller is given by:

$$G_c(S) = K_p + \frac{K_i}{S} \quad (23)$$

The PI controller reduces rise time and minimizes the steady-state error [16]. Peak overshoot, settling time, order, and type of the system will be increased [15]. It functions as a low pass filter. The output equations of the PI and PID controllers are given by:

$$u(t) = K_p e(t) + K_i \int e(t)\, dt \quad (24)$$

$$u(t) = K_p e(t) + K_i \int e(t)\, dt + K_d \frac{d}{dt}\, e(t) \quad (25)$$

A command speed ω^* is compared with the motor's speed ω_r and provides the change or error in speed $\Delta\omega$, which is given to the PI or PID controller to obtain the command torque component of stator current I_q^*. A limiter is used ahead of the controller to avoid decreased stability.

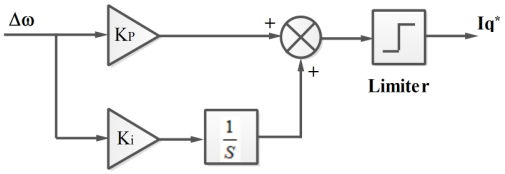

Fig. 1. PI controller block diagram.

The complete model block diagram of the PI controller of the PMSM-based BEV is illustrated in Figure 2. The command speed has been compared with the actual speed of the PMSM. An error speed signal is given to the PI controller to tune the signal with K_p and K_i values and provide the torque-producing current reference component I_q^*, which is essential to control the error speed by calculating the three-phase reference currents I_a^*, I_b^*, I_c^*. A Li-Ion battery with 100C capacity was used as the supply, which is converted into a three-phase supply voltage using a PWM inverter. The Li-Ion battery is operated with a current-controlled device with the feedback current provided by the PMSM. A sinusoidal PWM approach with the reference currents I_a^*, I_b^*, I_c^* corresponding to command speed and the actual currents I_a, I_b, I_c produced by the PMSM are collectively compared with a triangular reference signal to produce the gate pulses. Such desired gate pulses drive the three phase two-level inverter and will produce the three phase voltages for the PMSM. The characteristic equations of the PMSM building blocks are operated with inverter voltages and produce the instantaneous current, position, speed ω_e, and torque T_e of the motor. The PMSM will drive the vehicle's wheels through the transmission and differentials by considering the vehicle's dynamic losses.

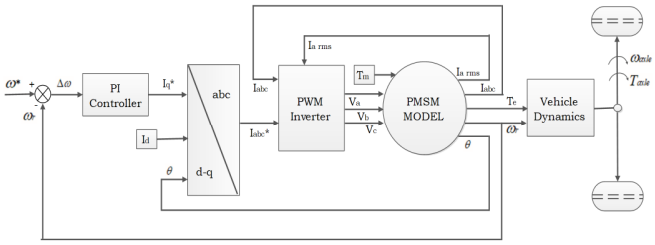

Fig. 2. Model analysis diagram of the speed control of the EV with PMSM drive using a PI controller.

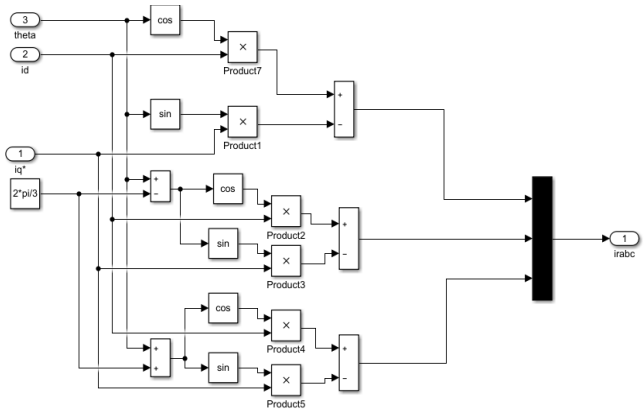

Fig. 3. Simulink model of dq to abc reference signals.

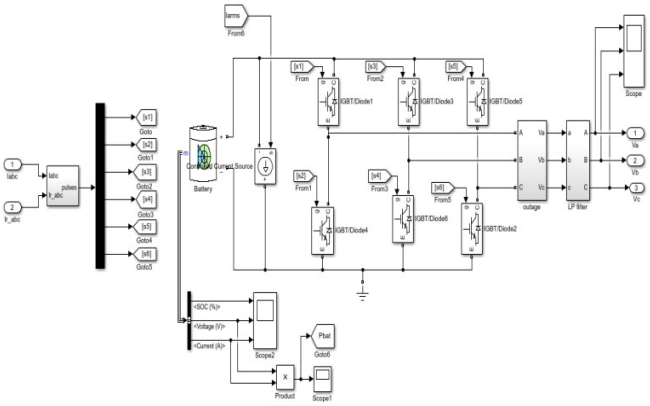

Fig. 4. Simulink model of the PWM inverter.

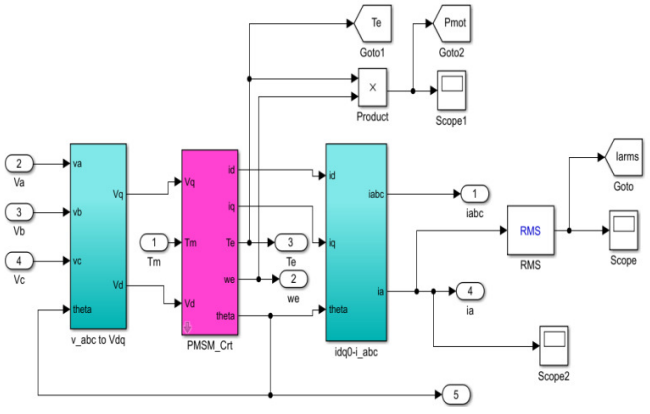

Fig. 5. Simulink model of PMSM.

Finally, the vehicle is operated smoothly with the required speed and torque. The performance results are discussed below.

In MATLAB Simulink version R2017a, the proposed work was simulated with the ode 23tb solver in continuous time mode. The design sub models like dq to abc reference, PWM inverter, PMSM model, and vehicle dynamic models are shown in Figures 3-7.

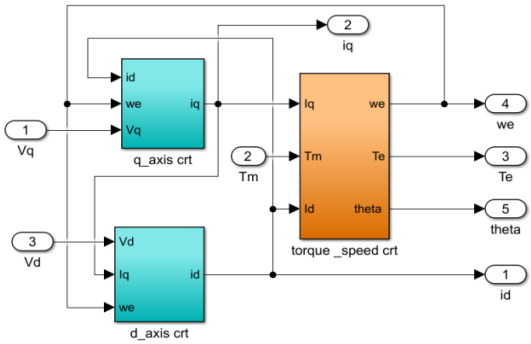

Fig. 6. Simulink model of PMSM internal characteristics.

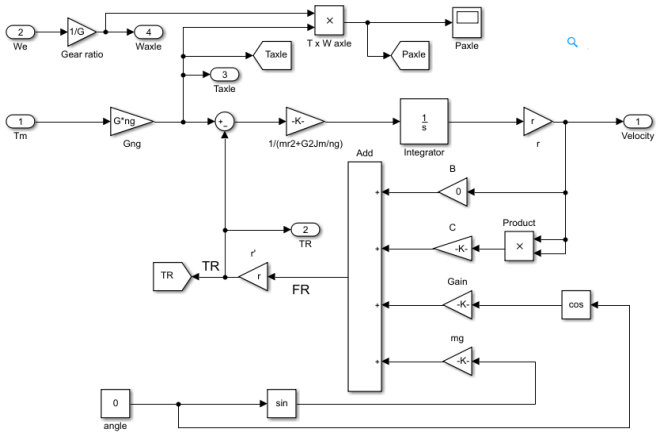

Fig. 7. Simulink model of vehicle dynamics (motor to wheels).

V. SIMULATION RESULTS

Simulations have been carried out with the PI and PID speed controllers for a 3-phase, 550Vdc, 1500rpm, 97.96Nm PMSM at a load torque of 80Nm and operating speed of 1500RPM or 157.079rad/sec. It can be observed that the rise time (90% of the command speed) is attained in 50.1ms with the PI controller, which is a better response than that of the PID controller. The motor speed stabilizes at a reference speed (with 2% tolerance) of 157.079rad/s in 70.1ms with the PID controller, which is slightly better performance than the one of the PI controller and with the steady state error of 0.0075rad/s or 0.0716rpm in both PI and PID controllers, as shown in Figure 8. The vehicle's acceleration (the speed at the wheels or the axle) was measured, and the time taken to reach the speed of 100Km/h is 48.1ms with the PI controller, which is superior to the performance of the PID controller, as shown in Figures 11-12. In the steady state, for a command torque of 80Nm, the torque developed by the PMSM is 80Nm.

TABLE III. PERFORMANCE RESULTS OF THE PROPOSED SYSTEM MODEL

		Motor side - speed			Axle side - speed
Controller type and its gain values	**Applied load (Nm)**	**Rise time required to reach 90% of final value (ms)**	**Settling time needed to get steady-state value with 2% tolerance (ms)**	**Steady state error**	**Time to reach 100Km/hr (ms)**
PI (Kp=0.35 Ki=16)	80	50.1	71.0	0.0075rad/s or 0.0716rpm	48.1
PID (Kp=0.35 Ki=16 Kd=0.01)	80	54.8	70.1	0.0075rad/s or 0.0716rpm	53.0

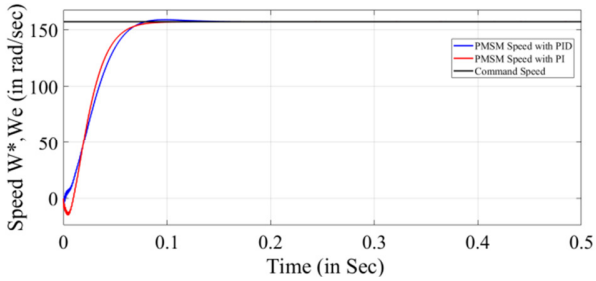

Fig. 8. Simulated speed responses with PI and PID controllers.

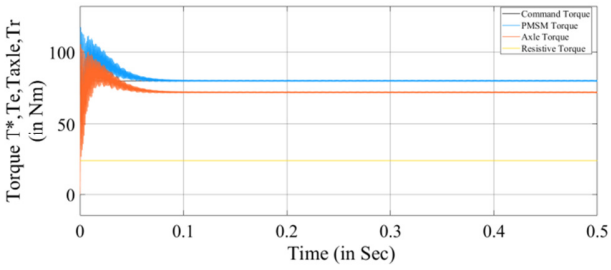

Fig. 9. Simulated torque responses with the PI controller.

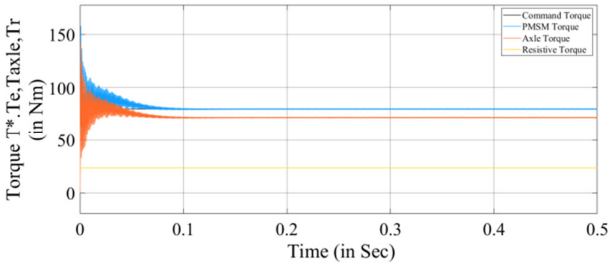

Fig. 10. Simulated torque responses with the PID controller.

The torque available at the wheel axle is 72.5Nm, with net tractive resistance loss of 7.5Nm due to rolling resistance, aerodynamic, and hill-climbing torque losses in both PI and PID controllers. The initial transient is higher in the PID controller than in the PI controller, as seen in Figures 9-10. The pulsating ripple torques are noticed due to the residual flux variation. The data of the mathematical model of the performance of the PMSM-based electric vehicle with PI and PID controller through MATLAB simulations are given in Table III.

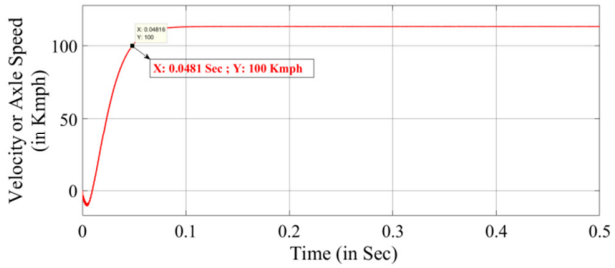

Fig. 11. Simulated vehicle acceleration pointing at the top speed of 100Km/hr with the PI controller.

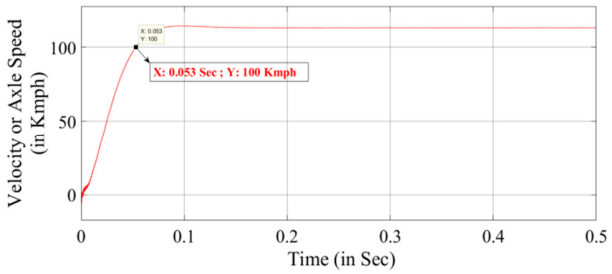

Fig. 12. Simulated vehicle acceleration pointing at top the speed of 100Km/hr with the PID controller.

VI. CONCLUSION

In this paper, the mathematical model of a vector controlled PMSM drive with PI and PID controllers as a propulsion system for an electric vehicle is developed, and its simulation results are presented. The results demonstrate that the PI controller achieves more robust tracking response of the command speed with less steady-state error than the PID controller. Good execution time and time are noted in the performance analysis. The vehicle acceleration at the wheel axle reached the desired value within a minimal time. The overall output responses of the model show that the vehicle can run smoothly with good static and dynamic performance characteristics with the PI controller.

REFERENCES

[1] C. C. Chan and K. T. Chau, "An overview of power electronics in electric vehicles," *IEEE Transactions on Industrial Electronics*, vol. 44, no. 1, pp. 3–13, Oct. 1997, https://doi.org/10.1109/41.557493.

[2] *Global Electric Vehicle Outlook 2022*. France: International Energy Agency, 2022.

[3] S. Morimoto, "Trend of permanent magnet synchronous machines," *IEEJ Transactions on Electrical and Electronic Engineering*, vol. 2, no. 2, pp. 101–108, 2007, https://doi.org/10.1002/tee.20116.

[4] R. N. Hajare and A. G. Thosar, "Modeling and Simulation of Permanent Magnet Synchronous Motor using MATLAB," vol. 7, no. 3, pp. 413–423, 2014.

[5] V. V. Patel, "Ziegler-Nichols Tuning Method," *Resonance*, vol. 25, no. 10, pp. 1385–1397, Oct. 2020, https://doi.org/10.1007/s12045-020-1058-z.

[6] E.-C. Shin, T.-S. Park, W.-H. Oh, and J.-Y. Yoo, "A design method of PI controller for an induction motor with parameter variation," in *IECON'03. 29th Annual Conference of the IEEE Industrial Electronics Society*, Roanoke, VA, USA, Aug. 2003, vol. 1, pp. 408–413, https://doi.org/10.1109/IECON.2003.1280015.

[7] "Electric and Hybrid Vehicles, Design Fundamentals [Book Review]," *IEEE Circuits and Devices Magazine*, vol. 21, no. 5, pp. 26–27, Sep. 2005, https://doi.org/10.1109/MCD.2005.1517392.

[8] J. Larminie and J. Lowry, *Electric Vehicle Technology Explained*, 2nd ed. Wiley, 2012.

[9] M. Y. Veeresh, V. N. B. Reddy, and R. Kiranmayi, "Range Estimation of Battery Electric Vehicle by Mathematical Modelling of Battery's Depth-of-Discharge," *International Journal of Engineering and Advanced Technology*, vol. 8, no. 6, pp. 3987–3992, Aug. 2019, https://www.doi.org/10.35940/ijeat.F8800.088619.

[10] M. Yildirim, M. C. Catalbas, A. Gulten, and H. Kurum, "Computation of the Speed of Four In-Wheel Motors of an Electric Vehicle Using a Radial Basis Neural Network," *Engineering, Technology & Applied Science Research*, vol. 6, no. 6, pp. 1288–1293, Dec. 2016, https://doi.org/10.48084/etasr.889.

[11] P. T. Giang, V. T. Ha, and V. H. Phuong, "Drive Control of a Permanent Magnet Synchronous Motor Fed by a Multi-level Inverter for Electric Vehicle Application," *Engineering, Technology & Applied Science Research*, vol. 12, no. 3, pp. 8658–8666, Jun. 2022, https://doi.org/10.48084/etasr.4935.

[12] P. Pillay and R. Krishnan, "Modeling of permanent magnet motor drives," *IEEE Transactions on Industrial Electronics*, vol. 35, no. 4, pp. 537–541, Aug. 1988, https://doi.org/10.1109/41.9176.

[13] C. Bowen, Z. Jihua, and R. Zhang, "Modeling and simulation of permanent magnet synchronous motor drives," in *ICEMS'2001. Proceedings of the Fifth International Conference on Electrical Machines and Systems*, Shenyang, China, Dec. 2001, vol. 2, pp. 905–908, https://doi.org/10.1109/ICEMS.2001.971825.

[14] A. Mansouri and T. Hafedh, "Torque Ripple Minimization and Performance Investigation of an In-Wheel Permanent Magnet Motor," *Engineering, Technology & Applied Science Research*, vol. 6, no. 3, pp. 987–992, Jun. 2016, https://doi.org/10.48084/etasr.644.

[15] J. C. Basilio and S. R. Matos, "Design of PI and PID controllers with transient performance specification," *IEEE Transactions on Education*, vol. 45, no. 4, pp. 364–370, Aug. 2002, https://doi.org/10.1109/TE.2002.804399.

[16] S. Mikkili and A. K. Panda, "SHAF for mitigation of Current harmonics with p-q and Id-Iq control strategies using both PI and Fuzzy Controllers," in *International Conference on Sustainable Energy and Intelligent Systems (SEISCON 2011)*, Chennai, India, Jul. 2011, pp. 358–362, https://doi.org/10.1049/cp.2011.0389.

AUTHORS PROFILE

M. Yerri Veeresh was born in Kurnool, India. He received the B.Tech (Electrical and Electronics Engineering) degree, M.Tech (Power Electronics and Electric Drives) from Jawaharlal Nehru Technological University Anantapur, India in 2009 and 2013 respectively. Presently, he is pursing his Ph.D. in the Department of Electrical Engineering, JNTU Anantapur and is also working as an Assistant Professor in the Santhiram Engineering College, Nandyal. His fields of interest include Electric Vehicles, Power Electronics and Drives, and Energy Sources.

V. Naga Bhaskar Reddy was born in Kurnool, India. He received the B.Tech (Electrical and Electronic Engineering) degree from the Bangalore University, Bangalore in 2000, M.Tech (Power Electronics and Drives) from the Bharath Institute of Higher Education Research (BIHER), Chennai, India in 2005. He attained his Doctoral degree from the Jawaharlal Nehru Technological University, Kakinada in 2012. He is currently a professor and the Head of the Department of Electrical and Electronic Engineering, R.G.M College of Engineering and Technology, Nandyal. His areas of interest are Power Electronics, Microcontrollers, and Power Electronic converters.

R. Kiranmayi received the B.Tech (Electrical and Electronic Engineering) degree, M.Tech., and Doctoral degree from Jawaharlal Nehru Technological University Anantapur, India in 1993, 1995, and 2013 respectively. She is presently working as a professor the Head of the Department of Electrical Engineering at JNTUA, Anantapuramu. She has published more than 40 research papers in international and national conferences and journals. Her areas of interest include Electrical Power Systems and Photo Voltaic Systems.